

## Similarity in silicate chemistry: trace elements in garnet solid solutions

Colin L. Freeman<sup>a</sup>, Mikhail Yu. Lavrentiev<sup>a,1</sup>, Neil L. Allan<sup>a,\*</sup>, John A. Purton<sup>b</sup>,  
Willem van Westrenen<sup>c</sup>

<sup>a</sup>School of Chemistry, University of Bristol, Cantock's Close, Bristol BS8 1TS, UK

<sup>b</sup>CLRC, Daresbury Laboratory, Warrington, Cheshire WA4 4AD, UK

<sup>c</sup>Faculty of Earth and Life Sciences, Vrije University, De Boelelaan 1085, 1081 HV Amsterdam, The Netherlands

Received 10 December 2004; accepted 27 January 2005

Available online 28 June 2005

### Abstract

Similarity concepts applied to the solid state are particularly useful when discussing the substitution of one cation by another. Here, we present a computational study of trace-element incorporation in a range of aluminosilicate garnet solid solutions. Atomistic simulations suggest trace elements are more soluble in a 50:50 pyrope ( $\text{Mg}_3\text{Al}_2\text{Si}_3\text{O}_{12}$ )–grossular ( $\text{Ca}_3\text{Al}_2\text{Si}_3\text{O}_{12}$ ) mixture, than in either end member, consistent with garnet-melt element partitioning experiments. Contrary to Goldschmidt's first rule, in this solid solution large trace-element cations may substitute for the small  $\text{Mg}^{2+}$  and large trace elements for  $\text{Ca}^{2+}$ . We examine also incorporation in a number of solid solutions involving combinations of pyrope, grossular, almandine ( $\text{Fe}_3\text{Al}_2\text{Si}_3\text{O}_{12}$ ) and spessartine ( $\text{Mn}_3\text{Al}_2\text{Si}_3\text{O}_{12}$ ) as end members. The results are analysed in terms of the likely ordering of the major divalent cations present in the solid solution and the size of the added trace element. © 2005 Elsevier B.V. All rights reserved.

**Keywords:** Solid-state chemistry; Solid solutions; Garnets; Non-ideality; Goldschmidt's rule

### 1. Introduction

Surprisingly, the language in common use by solid state and materials chemists rarely refers formally to similarity ideas. Despite this, similarity—as pioneered by Ramon Carbó-Dorca over many years—is as much a key concept in solid state as in molecular chemistry. Many problems encountered in this field are essentially *similarity* issues such as the ease of substitution of one atom or ion by another. This must necessarily depend on how similar are host and substituent. Relevant applications include ceramic processing, heterogeneous catalysis, high-temperature superconductivity and mineral geochemistry.

In this paper we consider garnet solid solutions and incorporation of trace elements in these solutions. We shall see that, as a consequence of cation ordering in

the solid solution, in some cases two ions, usually thought to be rather dissimilar, appear extremely similar.

### 2. Garnet solid solutions

The ease of incorporation of dopants and trace elements in oxides and minerals is basically a *similarity* problem. The substitution of one atom or ion by another depends on the similarity of host and substituent. The classic work of Goldschmidt [1] many years ago established controls for substitution in terms of the mismatch in valence and ionic radius between host ion and substituent. The *general* rule is that those dopants with the highest solubilities are most similar in radius and charge to the host ion they substitute for at any given crystal lattice site. Atomistic simulation techniques have provided a quantitative foundation for this via the calculation of the energies associated with trace element or dopant incorporation. In *end-member* compounds such as binary [2] and ternary oxides [3] and silicates [4], there is an approximately parabolic variation of calculated solution energy with ionic radius for any given

\* Corresponding author. Tel.: +44 117 9288308; fax: +44 117 9250612.  
E-mail address: n.l.allan@bris.ac.uk (N.L. Allan).

<sup>1</sup> On leave from Institute of Inorganic Chemistry, 630090 Novosibirsk, Russian Federation.

charge, and there is a minimum at a radius close to that of the host cation.

Non-ideal solid solutions present many challenges to the theoretician and trace-element incorporation in solid solutions has received little attention despite their obvious importance in areas ranging from ceramic technology to earth sciences. Most natural samples are solid solutions and this alone makes an evaluation of how solid solution formation influences trace-element energetics of particular interest. Models currently in place such as those invoking ‘forbidden zones’ [5] around a given dopant are crude and are often strikingly unsuccessful [6]. We chose to study aluminosilicate garnets since experimentally garnet-silicate melt element partitioning data indicate that some garnet solid solutions show anomalous trace-element partitioning behaviour [7] which is *not intermediate* between that of the pure end members.

We started our simulations of trace-element incorporation in garnets by comparing substitution at the dodecahedral X-sites (Fig. 1) of pyrope (Py,  $\text{Mg}_3\text{Al}_2\text{Si}_3\text{O}_{12}$ ), grossular (Gr,  $\text{Ca}_3\text{Al}_2\text{Si}_3\text{O}_{12}$ ) and pyrope–grossular solid solutions. We calculated the energetics of substitution of a number of divalent trace elements and of charge-balanced substitution by trivalent ions, using molecular mechanics techniques appropriate for the solid state. A conventional Born ionic model was used, in which integral ionic charges are assigned to all species, based on accepted chemical valence rules. Non-Coulombic two and three-body potentials were taken from a set used in previous work on a wide range of silicate minerals [8–10]. Polarisability of the oxide ion was partially accounted for using the shell model [11]. The Coulombic terms were calculated using the standard Ewald technique [12].

Static simulations of perfect lattices (i.e. without any trace elements present) give the lattice energy and crystal structure at zero pressure. In the static limit the lattice

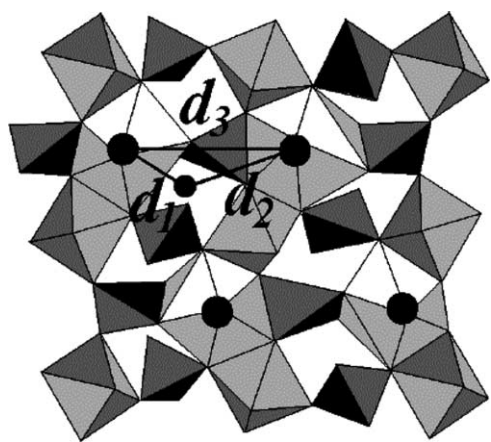


Fig. 1. The garnet structure, showing the  $\text{AlO}_6$  octahedra and the  $\text{SiO}_4$  tetrahedra. The first, second and third-nearest neighbour cation–cation distances are labelled. The third-nearest neighbour interaction ( $d_3$ ) between cations at the centre of two dodecahedra, as described in the text, is unusually repulsive for like cations.

structure is determined by the condition  $\partial U/\partial X_i$ , where  $U$  is the internal energy, neglecting vibrational contributions and the variables  $X_i$  the lattice vectors and basis atom coordinates which define the structure. No symmetry constraints were applied. As a test of the potential model, agreement between observed and computed structural parameters for the pyrope and grossular end members is very satisfactory. For example, the change in sign of the difference in O–O distances between unshared and shared  $\text{AlO}_6$  octahedral edges in pyrope and grossular is reproduced.

Simulations of solid solutions with Mg and Ca sites were carried out for compositions  $\text{Py}_{96}\text{Gr}_4$ ,  $\text{Py}_{50}\text{Gr}_{50}$ , and  $\text{Py}_4\text{Gr}_{96}$ .  $\text{Mg}^{2+}$  ions preserve largely pyrope-type and  $\text{Ca}^{2+}$  ions predominantly grossular-type environments even in  $\text{Py}_4\text{Gr}_{96}$  and  $\text{Py}_{96}\text{Gr}_4$ , respectively. Possible cation orderings in the solid solution were examined carefully. Unusually, as noted also in Ref. [6], the ordering energetics are dominated by the third nearest neighbour interaction between cations at the centre of two dodecahedra that share edges with the *same*  $\text{SiO}_4$  tetrahedron and which is repulsive for *like* cations ( $\text{Mg}^{2+}$ – $\text{Mg}^{2+}$  and  $\text{Ca}^{2+}$ – $\text{Ca}^{2+}$ ). Fig. 1 highlights this particular interaction in the garnet structure. The polyhedral network constrains the structure such that rigid-unit modes involving rigid rotations of the polyhedra are not permitted [6]. When an X-site cation is replaced all polyhedra can be distorted, with large distortions in the two  $\text{SiO}_4$  tetrahedra which share edges with the dodecahedron containing the new cation [6]. Mg–Mg and Ca–Ca third-nearest-neighbour pairs are energetically unfavourable with respect to Mg–Ca pairs in all three solid solution compositions studied.

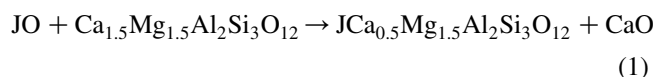
For  $\text{Py}_{50}\text{Gr}_{50}$ , a number of different arrangements of Mg and Ca atoms [13,14] were considered. The first of these (configuration 1) avoided all energetically unfavourable Mg–Mg and Ca–Ca third-nearest-neighbour cation pairs. In the remaining configurations the X-site had a range of different first, second and third-nearest cation neighbours. In other arrangements of the ions, the unit cell was doubled in one direction to make it possible to surround one X-site with two third-nearest cation neighbours of different types. Configuration 1 was the lowest in energy. Others were higher in energy by only 1 or 2  $\text{kJ mol}^{-1}$ , and so configurations containing ‘unfavourable’ Mg–Mg and Ca–Ca third-neighbour interactions are nevertheless energetically accessible at high temperatures.

These simulated structures were subsequently used as a basis for defect energy calculations. In every computational run, one or more defects were introduced into the crystal, e.g. for homovalent substitution, one divalent cation at the X-site of a perfect garnet lattice was replaced by one divalent trace-element cation. The total energy of the defective system was then minimised by allowing the surrounding ions to relax to accommodate the misfit cation(s), using the conventional two-region approach [15]. The inner region containing the defect(s) typically contained 400 ions. Final defect energies

after relaxation,  $U_{\text{def}}$ , were obtained at convergence. Although all simulations were in the static limit, defect energies in this limit have been shown to be in close agreement with defect enthalpies at elevated temperatures [16].

For composition  $\text{Py}_{50}\text{Gr}_{50}$  we examined substitutions for different local Mg–Ca distributions around the central X-site in order to study explicitly the effects of local X-site ordering on the energetics of trace-element incorporation. This included all possible nearest-neighbour and third-neighbour orderings (and combinations thereof), and a large number of second orderings.

Calculated solution energies  $U_{\text{sol}}$  of trace-element  $\text{J}^{2+}$  at a  $\text{Ca}^{2+}$  site in  $\text{Py}_{50}\text{Gr}_{50}$  are related to the equation



$$U_{\text{sol}} = U_{\text{def},f}(\text{J}) + U_{\text{latt}}(\text{CaO}) - U_{\text{latt}}(\text{JO})$$

where  $U_{\text{latt}}$  denotes the lattice energy of the appropriate binary oxide. Lattice energies for the binary oxides, obtained with the same inter-ionic potentials used for the garnet simulations, are listed in Ref. [10]. Analogous equations are easily obtained for substitution at a  $\text{Mg}^{2+}$  site and for other compositions.

The interatomic distances and orientations around a foreign trace element adjust *locally* to the most energetically favourable values, i.e. the new cation optimises its *local* environment. There are no rigid unit modes in the garnet structure and any tilting or rotation of a tetrahedron or octahedron in the framework to accommodate a trace-element cation in a resized dodecahedral X-site would require the same motion of all polyhedra, and the collective distortion thus involved would be high in energy. An alternative, lower in energy, is distortion, primarily of the tetrahedra and octahedra which are the direct neighbours of the trace element.

Small changes in environment in the solid solution lead to relatively large changes in  $U_{\text{def}}$ , and thus to the values of  $U_{\text{sol}}$ , which show some highly unusual features. The solution energies at some  $\text{Mg}^{2+}$  and  $\text{Ca}^{2+}$  sites are comparable! For example, the calculated solution energy for  $\text{Ba}^{2+}$  (the largest ion we consider) at a Mg site in  $\text{Py}_4\text{Gr}_{96}$  is comparable to that at a Ca site in grossular itself. The smallest ion we have considered is  $\text{Ni}^{2+}$  for which the lowest value of  $U_{\text{sol}}$  is at a  $\text{Ca}^{2+}$  site in  $\text{Py}_{96}\text{Gr}_4$  and this value is considerably lower than those for  $\text{Ni}^{2+}$  substitution in the end-members pyrope and in grossular (Fig. 2). This is totally at variance with Goldschmidt's first rule and any simple similarity measure based on ion size alone. In these garnet solid solutions small trace cations are predicted to substitute for the larger host ion ( $\text{Ca}^{2+}$ ) and large trace elements for the smaller host ion ( $\text{Mg}^{2+}$ ).

The key to this highly surprising behaviour in  $\text{Py}_{50}\text{Gr}_{50}$  appears to be the details of the ordering *locally* to the X-site. It is useful to begin with the trace-element  $\text{Ba}^{2+}$ . The first four

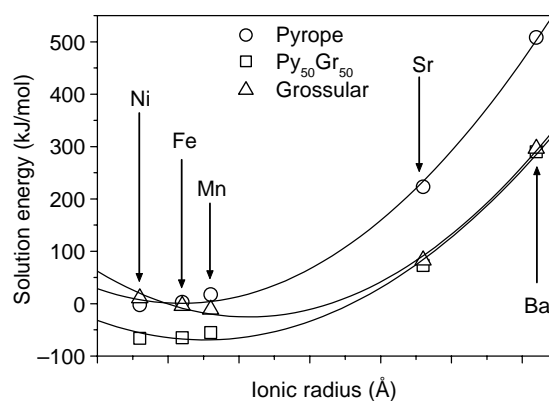


Fig. 2. Calculated solution energies for a range of divalent impurities in pyrope–grossular solid solutions. The arrows shown indicate that the solution energies in these solid solutions are substantially lower than would be expected from a linear interpolation between the end-member values (dashed line).

cation neighbours to the X-site influence the solution energy  $U_{\text{sol}}$  as for more dilute solutions: it is slightly larger if surrounded by larger ions. In addition the makeup of the third-nearest cation neighbour shell has a striking influence on defect energies and thus on solution energies. If substitution of the X-site cation removes an unfavourable third-neighbour interaction by introducing a size mismatch between the ions in this position, then defect and solution energies are lower, as the overall compression or extension of the tetrahedron between the two dodecahedra is reduced. For example,  $U_{\text{sol}}$  for replacement of a  $\text{Mg}^{2+}$  by  $\text{Ba}^{2+}$  is  $\approx 20\text{--}40 \text{ kJ mol}^{-1}$  lower depending on whether the first neighbours are all Mg or all Ca, with lower values for Ca neighbours. This is not unexpected since in that case the X-site will be slightly larger. However, the solution energy varies by as much as  $\approx 75 \text{ kJ mol}^{-1}$  depending on the nature of the third neighbour. Overall, the lowest solution energy of  $\text{Ba}^{2+}$  at an Mg site is  $\approx 250 \text{ kJ mol}^{-1}$  and at a Ca site  $\approx 290 \text{ kJ mol}^{-1}$ . It is interesting that it is more favourable to remove a  $\text{Mg}^{2+}\text{--Mg}^{2+}$  interaction than  $\text{Ca}^{2+}\text{--Ca}^{2+}$ , i.e. it is more favourable to replace  $\text{Mg}^{2+}\text{--Mg}^{2+}$  with  $\text{Ba}^{2+}\text{--Mg}^{2+}$  than to replace  $\text{Ca}^{2+}\text{--Ca}^{2+}$  with  $\text{Ba}^{2+}\text{--Ca}^{2+}$ . This appears to be due to the small size of the  $\text{Mg}^{2+}$  ion which is effectively too small for the X-site, and ab initio calculations to explore this are currently in progress.

These are striking results since they suggest the favoured substitution site for the large  $\text{Ba}^{2+}$  in  $\text{Py}_{50}\text{Gr}_{50}$  is not necessarily a  $\text{Ca}^{2+}$  site as expected from Goldschmidt's first rule [1]. Substitution in  $\text{Py}_{50}\text{Gr}_{50}$  is possible at a Mg site depending on the local environment of this site. For comparison [10], the solution energy of  $\text{Ba}^{2+}$  in pure pyrope is  $462 \text{ kJ mol}^{-1}$  and in grossular  $266 \text{ kJ mol}^{-1}$ . As shown in Fig. 2, the variation in calculated solution energy along the pyrope–grossular join is thus non-linear, with values for  $\text{Py}_{50}\text{Gr}_{50}$  lower than those for either end member. In addition, the possibility of substitution at more than one sublattice will lower the free energy of substitution

because of the larger configurational entropy change accompanying the disordering of two sublattices rather than only one. All these factors result in a predicted higher solubility of  $\text{Ba}^{2+}$  (and  $\text{Sr}^{2+}$ ) in  $\text{Py}_{50}\text{Gy}_{50}$  than that expected from an interpolation between the end-member compounds.

A similar set of arguments can be used to rationalise the defect energies for  $\text{Ni}^{2+}$  remembering that  $\text{Ni}^{2+}$  is only slightly smaller than  $\text{Mg}^{2+}$ . Introducing a  $\text{Ni}^{2+}$  at an X-site where both third neighbours are  $\text{Ca}^{2+}$  is favoured relative to a site with two  $\text{Mg}^{2+}$  third neighbours due to the removal of the effective repulsion between an ion ( $\text{Ni}^{2+}$ ) and a third neighbour ( $\text{Mg}^{2+}$ ) similar in size. This is sufficiently important for the lowest solution energy for  $\text{Ni}^{2+}$  to be for replacement of a  $\text{Ca}^{2+}$  rather than substitution of a  $\text{Mg}^{2+}$ . Once more this is not in line with ion size considerations. Fig. 2 also shows results for  $\text{Fe}^{2+}$  and  $\text{Mn}^{2+}$  in  $\text{Py}_{50}\text{Gy}_{50}$ . These lie between  $\text{Mg}^{2+}$  and  $\text{Ca}^{2+}$  in size but are closer to  $\text{Mg}^{2+}$ . Like  $\text{Ni}^{2+}$ , these ions are predicted to substitute at a  $\text{Ca}^{2+}$  site which possesses two  $\text{Ca}^{2+}$  third neighbours and solution energies are lower than in either of the end-member compounds. This proposed link between dopant distribution and local Ca–Mg ordering should be testable using EXAFS.

Fig. 3 plots the calculated solution energy as a function of Shannon ionic radius [17] and serves as a useful summary of our overall conclusions.  $\text{Ni}^{2+}$ ,  $\text{Fe}^{2+}$ ,  $\text{Mn}^{2+}$ ,  $\text{Sr}^{2+}$  and  $\text{Ba}^{2+}$  all appear more soluble in  $\text{Py}_{50}\text{Gy}_{50}$  than in either the pyrope or the grossular end member. A large ion may substitute preferentially for a  $\text{Mg}^{2+}$  (with two  $\text{Mg}^{2+}$  third neighbours) rather than a  $\text{Ca}^{2+}$  and a small ion may substitute preferentially for a  $\text{Ca}^{2+}$  (with two  $\text{Ca}^{2+}$  third neighbours) rather than for a  $\text{Mg}^{2+}$ . Thus, a simple similarity index in terms of an optimum cation radius transferable from system to system, as suggested by Goldschmidt, breaks down for the garnet solid solution. The minimum in the curve for  $\text{Py}_{50}\text{Gy}_{50}$  in Fig. 3 lies between  $\text{Ca}^{2+}$  and  $\text{Mg}^{2+}$ . An explanation is also provided for the anomalous trace-element partitioning behaviour of the solid solution [7] since the net result from the

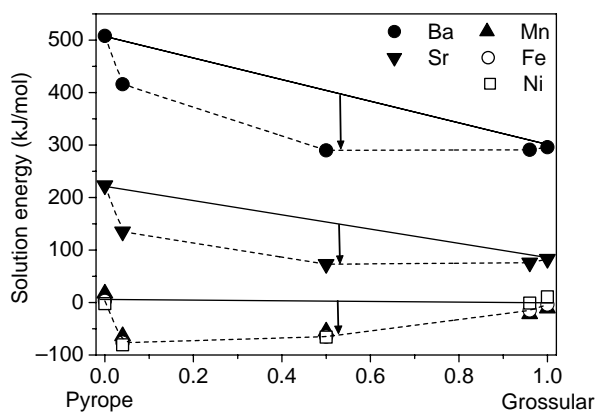


Fig. 3. Solution energies as a function of ionic radius for pyrope, grossular and  $\text{Py}_{50}\text{Gr}_{50}$ .

partitioning perspective is a solution energy vs. ionic radius curve with a lower curvature than for either end member, consistent with experiment.

We have only examined heterovalent substituents briefly. For trivalent trace cations  $\text{J}^{3+}$ , a  $\text{Li}^{+}$  cation was placed simultaneously on the adjacent (nearest neighbour) X-site [10] to maintain charge-balance. Analogous equations can be constructed for the partitioning process of trivalent trace elements (Eqs. 4 and 7 in Ref. [10]), assuming that the local environments of  $\text{J}^{3+}$  and  $\text{Li}^{+}$  are equivalent to their environments in the corresponding solid binary oxides ( $\text{J}_2\text{O}_3$  and  $\text{Li}_2\text{O}$ ). Since the nature of the charge-balancing substitution is an additional factor that influences the resulting energies, there are even more local configurations to examine. Replacement of a Mg by a La could be charge-balanced by the insertion of a Li in place of another Mg or Ca in  $\text{Py}_{50}\text{Gr}_{50}$ , while in pure pyrope Li can only replace Mg. Results show the most energy-efficient charge-balancing mechanism involves the replacement of another Ca with Li, and that overall the solution energy variation is similar to that for the divalent elements, with solution energies lower in the mixed garnet than in either end member.

Hence, although *structurally* the Ca and Mg sites clearly remain distinct in the solid solution, *energetically* they may appear equivalent depending on the local environment, which we have shown to be dominated by the four nearest X-sites. EXAFS data [18] on the local relaxation around  $\text{Yb}^{3+}$  in pure Py and Gr confirm the structural relaxation around trace elements at the X-site is extremely localised.

### 3. Other solid solutions

To what extent are the same trends evident in other garnet solid solutions? To address this question we have repeated the calculations for other garnet solid solutions, involving combinations of pyrope or grossular with almandine ( $\text{Fe}_3\text{Al}_2\text{Si}_3\text{O}_{12}$ ) or spessartine ( $\text{Mn}_3\text{Al}_2\text{Si}_3\text{O}_{12}$ ) as end members. The eight-fold coordinated ionic radii [17] of  $\text{Mg}^{2+}$ ,  $\text{Fe}^{2+}$ ,  $\text{Mn}^{2+}$  and  $\text{Ca}^{2+}$  are 0.89, 0.92, 0.96 and 1.12 Å, respectively, so that all these solutions involve cations with a smaller size mismatch than the pyrope–grossular solid solution itself.

For each 50:50 composition we calculated solution energies for five trace elements ( $\text{Ni}^{2+}$ ,  $\text{Sr}^{2+}$  and  $\text{Ba}^{2+}$  and the two members of the set  $\text{Mg}^{2+}$ ,  $\text{Ca}^{2+}$ ,  $\text{Fe}^{2+}$  and  $\text{Mn}^{2+}$  that were not major elements in each particular case). For grossular–almandine, where the size-mismatch between  $\text{Ca}^{2+}$  and  $\text{Fe}^{2+}$  is almost as large as in pyrope–grossular, the calculated solution energies show similar trends as for pyrope–grossular itself. The (smaller)  $\text{Ni}^{2+}$ ,  $\text{Mg}^{2+}$  and  $\text{Mn}^{2+}$  preferentially substitute for  $\text{Ca}^{2+}$ , the (larger)  $\text{Ba}^{2+}$  and  $\text{Sr}^{2+}$  for  $\text{Fe}^{2+}$ . In all cases substitution is at an X-site where the third neighbours are the same species as at the substitution site. Substitution removes the unfavourable

third-neighbour interaction between ions of the same size, e.g.  $\text{Ba}^{2+}$  substitutes at a  $\text{Fe}^{2+}$  site with two  $\text{Fe}^{2+}$  as third neighbours, replacing the  $\text{Fe}^{2+}$ – $\text{Fe}^{2+}$  interaction with a  $\text{Ba}^{2+}$ – $\text{Fe}^{2+}$  interaction.

In the pyrope–almandine and pyrope–spessartine solid solutions, where the size-mismatch is smaller, the lowest solution energies of all five trace elements were for substitution at a  $\text{Mg}^{2+}$  site. In these two cases,  $\text{Ni}^{2+}$  is now behaving in line with Goldschmidt's rule, while the larger ions ( $\text{Ca}^{2+}$ ,  $\text{Sr}^{2+}$ ,  $\text{Ba}^{2+}$ ) are still deviating from this rule in their preference for the smaller cation  $\text{Mg}^{2+}$ . In these examples, we are again seeing the avoidance of similarly sized cation neighbours. The larger cations always substitute such that a  $\text{Mg}^{2+}$ – $\text{Mg}^{2+}$  first–third neighbour interaction is removed.

In contrast, in the grossular–spessartine solid solution all the trace elements are predicted to substitute for  $\text{Ca}^{2+}$ . The larger cations ( $\text{Sr}^{2+}$ ,  $\text{Ba}^{2+}$ ) are now substituting in line with Goldschmidt's rule and the  $\text{Ca}^{2+}$  site with the lowest solution energy has one  $\text{Mn}^{2+}$  and one  $\text{Ca}^{2+}$  third-nearest neighbour; the third-nearest neighbour interactions appear less important here. The smaller cations are deviating from the rule in their preference for the larger cation  $\text{Ca}^{2+}$ . They substitute at an X-site with two  $\text{Ca}^{2+}$  as third-nearest neighbours removing the  $\text{Ca}^{2+}$ – $\text{Ca}^{2+}$  interaction.

It is interesting to consider the different cases when Goldschmidt's rule takes precedence over the removal of unfavourable third-neighbour interactions. This is clearly most important when the size-mismatch between the major cations in the solid solution is largest (grossular–pyrope and grossular–almandine). But the smallest size mismatch is for the pyrope–almandine solution where all the cations except  $\text{Ni}^{2+}$  disobey Goldschmidt's rule and the removal of the third-neighbour interaction is dominant. The size mismatch is greater in grossular–spessartine but only the smaller cations show anti-Goldschmidt behaviour. It is clear that the actual

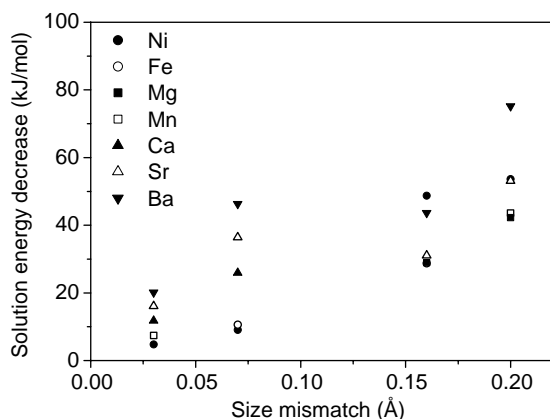


Fig. 4. The difference between the calculated solution energies in 50:50 garnet solid solutions and that predicted from a linear interpolation between the end members ('solution energy decrease') as a function of the size mismatch between the major cations present in the solid solution. All cations are *more* soluble than an interpolation between the end members would indicate.

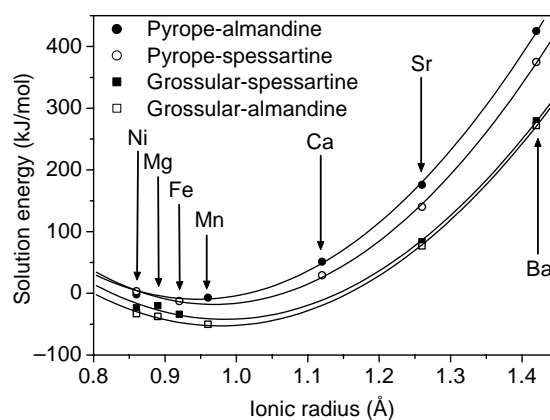


Fig. 5. Solution energies as a function of trace-element ionic radius for the 50:50 pyrope–almandine, pyrope–spessartine, grossular–spessartine and grossular–almandine solid solutions.

sizes of the cations as well as their size-mismatch determine the site preference for the trace element.

The variations in calculated solution energies along the joins are all non-linear and the 50:50 solution energies are lower than for either end member; all 2+ trace-element cations are more soluble in the solid solution than in the end members. This deviation from a linear trend in general increases with size-mismatch as is clear from Fig. 4. The curves in Fig. 5 show the variation in the calculated trace-element solution energy for each solid solution. Note that the minimum in each curve occurs at an ionic radius intermediate between that of the major cations.

#### 4. Conclusions

Under certain circumstances two ions, conventionally taken to be rather *dissimilar*, can appear to be extremely *similar*. Any similarity measure would need to take account of more than the size and charge of an individual ion. Our example shows the extra complexity of extending similarity ideas to solids, since they illustrate well the importance of the local structural environment of each ion and the complexities of the defect chemistry of the systems of interest. It will be of interest in the future to consider similarity measures for solids similar to those used in the Carbó molecular similarity index, involving integrals of functions of the electron density. There remains much to do in extending similarity concepts to the solid state and ultimately similarity measures that relate to condensed phases will need to take account of free rather than static energies.

#### References

- [1] V.M. Goldschmidt, J. Chem. Soc. (Lond.) 140 (1937) 655.
- [2] W.C. Mackrodt, R.F. Stewart, J. Phys. C: Solid State Phys. 12 (1979) 5015.

- [3] N.L. Allan, W.C. Mackrodt, *Adv. Solid State Chem.* 3 (1993) 221.
- [4] N.L. Allan, J.D. Blundy, J.A. Purton, M.Yu. Lavrentiev, B.J. Wood, Trace element incorporation in minerals and melts, in: C.A. Geiger (Ed.), *Solid Solutions in Silicate and Oxide Systems*, in: G. Papp and T.G. Weiszbürg (Eds.), *European Mineralogical Union Notes in Mineralogy*, series, vol. 3, Eötvös University Press, Budapest, 2001, pp. 251–302 (Chapter 11).
- [5] J.T. Iiyama, *Bull. Soc. Fr. Mineral. Cristallogr.* 97 (1974) 143; R.C. Newton, B.J. Wood, *Am. Mineral.* 65 (1980) 733.
- [6] A. Bosenick, M.T. Dove, C.A. Geiger, *Phys. Chem. Miner.* 27 (2000) 398.
- [7] W. van Westrenen, J.D. Blundy, B.J. Wood, *Am. Mineral.* 84 (1999) 838.
- [8] J.A. Purton, N.L. Allan, J.D. Blundy, E.A. Wasserman, *Geochim. Cosmochim. Acta* 60 (1996) 4977.
- [9] J.A. Purton, N.L. Allan, J.D. Blundy, *Geochim. Cosmochim. Acta* 61 (1997) 3927.
- [10] W. van Westrenen, N.L. Allan, J.D. Blundy, J.A. Purton, J. Wood, *Geochim. Cosmochim. Acta* 64 (2000) 1629.
- [11] B.G. Dick, A.W. Overhauser, *Phys. Rev.* 112 (1958) 90.
- [12] P.P. Ewald, *Ann. Phys.* 64 (1921) 253.
- [13] W. van Westrenen, N.L. Allan, J.D. Blundy, M.Yu. Lavrentiev, B.R. Lucas, J.A. Purton, *Chem. Commun.* 2003; 786.
- [14] W. van Westrenen, N.L. Allan, J.D. Blundy, M.Yu. Lavrentiev, B.R. Lucas, J.A. Purton, *Phys. Chem. Miner.* 30 (2003) 217; for a detailed Monte Carlo study of pyrope–grossular solid solutions see M.Yu. Lavrentiev, C.L. Freeman, W. van Westrenen, N.L. Allan, J.A. Purton, to be published.
- [15] C.R.A. Catlow, W.C. Mackrodt, in: C.R.A. Catlow, W.C. Mackrodt (Eds.), *Computer Simulation of Solids*, Springer, Berlin, 1982.
- [16] M.B. Taylor, G.D. Barrera, N.L. Allan, T.H.K. Barron, W.C. Mackrodt, *Faraday Discuss.* 106 (1997) 377.
- [17] R.D. Shannon, *Acta Cryst. A* 32 (1976) 751.
- [18] S. Quartieri, G. Antonioli, C.A. Geiger, G. Artioli, P.P. Lottici, *Phys. Chem. Miner.* 26 (1999) 251.